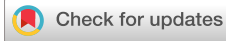


RESEARCH ARTICLE | OCTOBER 23 2003

## Communication with a chaotic traveling wave tube microwave generator

Vasily Dronov; Matthew R. Hendrey; Thomas M. Antonsen, Jr.; Edward Ott



Chaos 14, 30–37 (2004)

<https://doi.org/10.1063/1.1622352>



View  
Online



Export  
Citation

CrossMark

### AIP Advances

Why Publish With Us?

-  **25 DAYS**  
average time to 1st decision
-  **740+ DOWNLOADS**  
average per article
-  **INCLUSIVE**  
scope

[Learn More](#)



# Communication with a chaotic traveling wave tube microwave generator

Vasily Dronov,<sup>a)</sup> Matthew R. Hendrey, Thomas M. Antonsen, Jr.,<sup>b)</sup> and Edward Ott<sup>b)</sup>

*Institute for Research in Electronics and Applied Physics, and Department of Electrical and Computer Engineering, University of Maryland, College Park, Maryland 20742*

(Received 12 January 2003; accepted 6 September 2003; published online 23 October 2003)

Traveling wave tubes (TWTs) are vacuum electronic amplifiers (see Beck, Gittins, and Pierce) that are commonly used for communication in the centimeter wavelength range. Increasing demand for high data flow in wireless communication systems (satellite communication systems are a good example) raises needs for making TWT's more compact and efficient. Motivated by this we suggest a scheme in which a TWT with feedback is operated in a highly nonlinear regime where the device behaves chaotically. The chaos is controlled using small controls. Then, at the receiving end a receiving TWT synchronizes to the chaotic transmitter and amplifies the received signal with nearly no distortion. Results on numerical simulations of the proposed scheme are reported and used to evaluate its effectiveness. © 2004 American Institute of Physics. [DOI: 10.1063/1.1622352]

**In this paper we consider a scheme for microwave communication where we are attempting to use an alternative means of “modulation” for the encoding of binary information. Both the transmitter and receiver in our scheme use a traveling wave tube (TWT), a high power vacuum electronic amplifier commonly used in communication satellites, etc. In our scheme, however, TWT behaves chaotically and modulation is achieved by means of controlling chaotic dynamics of the tube. The main advantage of such a scheme is an increase in power efficiency of the transmitting amplifier. We believe that this work may be relevant in applications where the key requirements for communication system design are compactness and power efficiency. We present a model for the proposed communication scheme as well as results of numerical simulations of the model equations.**

## I. INTRODUCTION

In the system we envision, the signal sent by the transmitter is generated by a traveling wave tube (TWT) oscillator<sup>1–3</sup> operating in the chaotic regime. That is, under the supposed operating conditions, the TWT naturally produces a narrow band microwave signal with temporally chaotic phase and amplitude variations. We show that, if suitable small perturbations are applied to the TWT, the symbolic dynamics of the chaotic TWT can be controlled. Following the idea of Hayes *et al.*,<sup>4,5</sup> the information being transmitted is encoded in the controlled symbolic dynamics of the chaos.

The detection of the signal at the receiver can be accomplished by use of a replica of the transmitter's chaotic TWT oscillator. The small received signal is amplified by the replica receiver system through the phenomenon of synchronization of chaos.<sup>6</sup> This provides a potentially simple, cheap, and compact amplifier for the detector system, which is only

possible because the original signal was produced by a chaotic system. A notable feature of this scheme is that, in the ideal case, the signal amplification is in principal distortionless, even though the process is nonlinear (the nature of distortionless amplification is explained in Sec. V). In applications where the benefits of receiver simplicity and compactness are paramount (e.g., satellite-based communication), our scheme may provide an advantage.

In Sec. II we describe a model for a TWT feedback oscillator. In Sec. III we investigate this model through numerical simulations, display its chaotic behavior and characterize this behavior. In Sec. IV we discuss how, following the scheme of Refs. 4 and 5, information can be encoded in the TWT oscillator output through control of the symbolic dynamics of the chaos. In Sec. V we discuss the possibility of using the phenomenon of synchronization of chaotic systems for the purpose of efficiently amplifying and retransmitting a chaotic signal of the type discussed in Sec. IV. A noise analysis of such a chaos-based communication system is given in Sec. VI. In Sec. VII we present further discussion and summarize our conclusions.

Finally, we wish to emphasize that our motivation for considering TWT oscillator operation in the chaotic regime is the possibility of attaining improved power efficiency and device compactness. In particular, unlike some other work using chaos in communications,<sup>7,8</sup> secrecy is not one of our goals.

## II. THE MODEL

In this section we review a model for the nonlinear operation of a TWT which can be made to oscillate by adding feedback. We model the TWT in the following way. Assume that the signal at the input is  $A_{in}e^{i\omega_c t}$  where  $A_{in}(t)$  is the complex envelope of the signal and  $\omega_c$  is the carrier or reference frequency. The linear behavior of the tube is modeled as a first-order bandpass filter with the bandwidth  $2\Delta\omega$ , centered near the carrier frequency. The linear gain of the filter is  $G_L$ . Nonlinearity arises due to power saturation as the electron beam bunches toward the output end of the TWT. A

<sup>a)</sup>Present address: Comsat Labs, Division of ViaSat, 22300 Comsat Dr., Clarksburg, Maryland 20871.

<sup>b)</sup>Also at the Department of Physics.

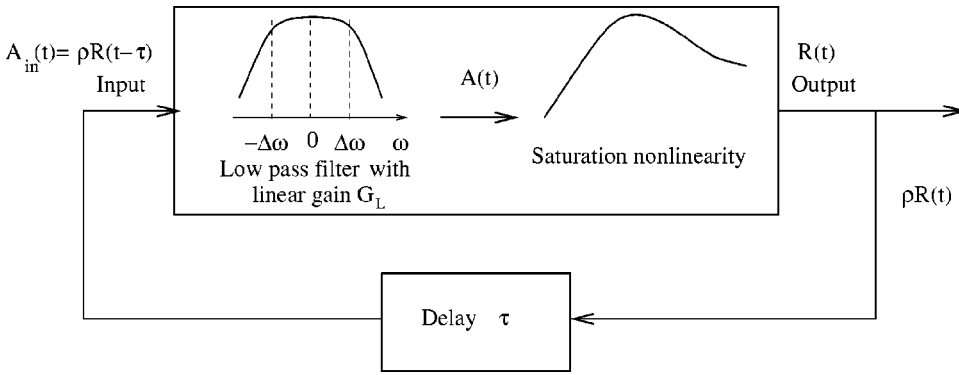


FIG. 1. Schematic of the free-running chaotic oscillator.

small fraction  $\rho$  of the output is then fed back into the input through a feedback line with delay time  $\tau$ . Performing a frequency shift  $\omega \rightarrow \omega - \omega_c$  we translate the analysis to low frequency (i.e.,  $A_{in} e^{i\omega_c t} \rightarrow A_{in}$ ) so that the time variation of the complex variable  $A_{in}$  represents the slow amplitude and phase modulation of  $\text{Re}[A_{in} e^{i\omega_c t}]$ . A schematic diagram of the model in this low-frequency representation is shown in Fig. 1.

The input  $\bar{A}_{in}(\omega)$  and the output  $\bar{A}(\omega)$  of the first-order low-pass filter with the bandwidth  $2\Delta\omega$  are related by

$$\bar{A}(\omega) = \frac{G_L \bar{A}_{in}(\omega)}{1 + i\omega/\Delta\omega},$$

and, therefore,

$$\bar{A}_{in}(\omega) = \frac{\bar{A}(\omega)(1 + i\omega/\Delta\omega)}{G_L},$$

in the frequency domain, and

$$A_{in}(t) = \left[ (\Delta\omega)^{-1} \frac{d}{dt} + 1 \right] \frac{A(t)}{G_L},$$

in the time domain. In general the frequency dependence of the linear transfer function for a TWT is more complicated than a simple first-order bandpass filter. We adopt the first-order bandpass filter here because that is the simplest model giving a nonzero memory time. Since TWT amplifiers are broadband, our model can be realized by inserting a narrow band first-order filter in the signal path. The TWT output (Fig. 1) is

$$R(t) = A(t) \frac{e^{i\eta|A(t)|^2}}{1 + |A(t)|^2}, \quad (1)$$

where the term  $[\exp(i\eta|A(t)|^2)][1 + |A(t)|^2]^{-1}$  models the nonlinearity of the TWT with  $\eta$  being a parameter characterizing the quadratic phase nonlinearity, and the coefficient of  $|A(t)|^2$  in the denominator of (1) can be set to 1 using a suitable normalization of  $A(t)$ . This model of the nonlinearity is one of a class of models due to Saleh<sup>9</sup> which have been used in the community<sup>10</sup> to simulate communications systems with TWT's. Since  $A_{in}(t) = \rho R(t - \tau)$ , the equation for  $A(t)$  becomes

$$\frac{dA(t)}{dt} + A(t) = kA(t - \tau) \frac{e^{i\eta|A(t - \tau)|^2}}{1 + |A(t - \tau)|^2}, \quad (2)$$

where  $k$  is the loop gain,  $k = \rho G_L$ , and the bandwidth  $\Delta\omega$  has been normalized to unity by means of a rescaling of the time variables, i.e.,  $t \rightarrow t\Delta\omega$  and  $\tau \rightarrow \tau\Delta\omega$ .

Note that our modeling of a TWT as consisting of linear and nonlinear stages (as illustrated in Fig. 1) is only an approximation and that such a sharp decomposition does not truly exist. Nevertheless, it has been found<sup>9,10</sup> that Eq. (2) is very effective at modeling real TWT experiments. Also note that the model variable  $A(t)$ , the output of the fictitious linear stage, is not a measurable physical quantity, but that  $R(t)$ , given in Eq. (1) in terms of  $A(t)$ , does represent a measurable physical quantity.

It is also important to mention that, while a wide variety of TWT models exist<sup>3,9,10</sup> with varying complexity,<sup>11-13</sup> the unique property of our model is that it is perhaps the simplest that is able to describe the behavior of a TWT oscillator with feedback.

### III. CHAOTIC BEHAVIOR

The right-hand side of Eq. (2) contains a delayed argument  $A(t - \tau)$ . Thus (2) is an infinite dimensional dynamical system [to evolve  $A(t)$  forward from  $t = \tau$ , we must specify the *function*  $A(t)$  in  $0 \leq t \leq \tau$ ]. The dynamics of the system can, however, be finite dimensional or even low dimensional. In particular, the system state may asymptote to a low dimensional subset of the infinite dimensional state space. This subset is called an attractor. We are interested in the case where the system motion on the attractor is chaotic. In the case of low dimensional chaotic dynamics, it is often feasible to find a phase space partition and the corresponding symbolic dynamics for the chaotic attractor. However, there is no common recipe for finding a parameter set that makes the dynamics chaotic and low dimensional. A powerful tool that can be helpful in this situation is the set of Lyapunov exponents for the system. Our goal is to arrive at a situation where the largest Lyapunov exponent is positive (yielding chaos) while others are either zero or negative (in order to provide contraction of the flow in the directions normal to the expansion direction).

In order to compute the Lyapunov exponents we consider an infinitesimal variation from  $A(t)$ , denoted  $\delta A(t)$ . Equation (2) yields the following linearized equation for  $\delta A$ :

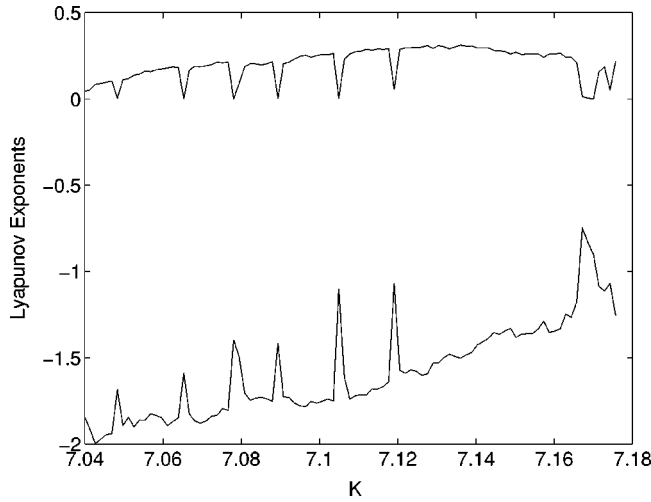


FIG. 2. Lyapunov exponents as functions of  $k$ ,  $\tau=0.530$  and  $\eta=1.0$ .

$$\begin{aligned}
 & \frac{d[\delta A(t)]}{dt} + \delta A(t) \\
 &= k \frac{e^{i\eta|A(t-\tau)|^2}}{1+|A(t-\tau)|^2} \left[ \delta A(t-\tau) + A(t-\tau) \right. \\
 & \quad \times \left\{ i\eta - \frac{1}{1+|A(t-\tau)|^2} \right\} \{ A(t-\tau) \delta A^*(t-\tau) \\
 & \quad \left. + A^*(t-\tau) \delta A(t-\tau) \right\}, \quad (3)
 \end{aligned}$$

where  $\delta A^*$  is the complex conjugate of  $\delta A$ . In order to compute the first  $N$  exponents, we start with  $N$  unit norm orthogonal functions  $\delta A_i = u_i$  on the interval  $[0, \tau]$ , i.e.,

$$\begin{aligned}
 (u_i(t), u_i(t)) = \|u_i(t)\|^2 &= \frac{1}{\tau} \int_0^\tau \{ \text{Re}[u_i(t)] \text{Re}[u_i(t)] \\
 & \quad + \text{Im}[u_i(t)] \text{Im}[u_i(t)] \} dt = 1,
 \end{aligned}$$

$$\begin{aligned}
 (u_i(t), u_j(t)) &= \frac{1}{\tau} \int_0^\tau \{ \text{Re}[u_i(t)] \text{Re}[u_j(t)] \\
 & \quad + \text{Im}[u_i(t)] \text{Im}[u_j(t)] \} dt = 0, \quad \text{for } i \neq j.
 \end{aligned}$$

Following the procedure described, for example, in Ref. 14, p. 148, we integrate (3) with these initial conditions and periodically use a Gram–Schmidt algorithm to renormalize the functions  $\delta A_i$ , keeping them orthogonal as we integrate the flow forward in time. The  $i$ th Lyapunov exponent  $\lambda_i$  is computed as the average rate of exponential growth of the norm of the function  $\delta A_i(t)$ , i.e.,  $\lambda_i = \lim_{T \rightarrow \infty} \times (1/T) \log[\|\delta A_i(T)\|/\|\delta A_i(0)\|]$ , where the subscript label  $i$  is chosen so that  $\lambda_1 \geq \lambda_2 \geq \lambda_3 \geq \dots$ .

Figure 2 shows results of a computation of the first four Lyapunov exponents for  $\tau$  and  $\eta$  fixed and  $k$  varied. Only the positive and least negative exponents are plotted. Two other exponents are identically zero by virtue of the invariance of Eq. (2) under time translation and under a change of the

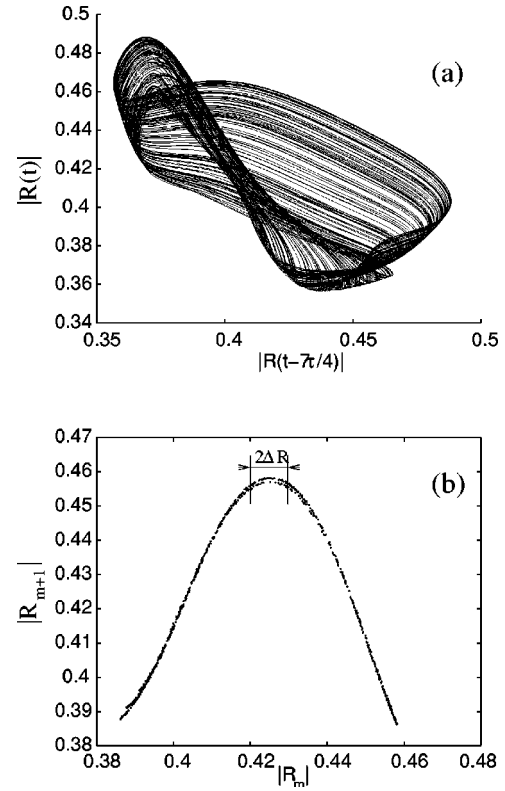


FIG. 3. (a) Uncontrolled attractor for  $k=7.142$ ,  $\tau=0.530$  and  $\eta=1.0$ . (b) Return map for the same attractor using the surface of section  $|R(t-7\tau/4)|=0.425$ .

phase of  $A$  [i.e.,  $A \rightarrow A \exp(i\varphi)$ , where  $\varphi$  is a constant]. In Fig. 3(a) we show  $|R(t)|$  versus  $|R(t-7\tau/4)|$  for  $k=7.142, \tau=0.530, \eta=1.0$ . Figure 3(b) shows the return map  $|R_{m+1}| = f(|R_m|)$ , where  $|R_m|$  is the value of  $|R(t)|$  at the  $m$ 'th passage of  $|R(t-7\tau/4)|$  through the value 0.425 going from left to right [i.e.,  $d|R(t-7\tau/4)|/dt > 0$  at  $t=t_m$ ]. We note that the return map is nearly one dimensional, indicating that the dimension of the attractor in Fig. 3(a) is near (but slightly bigger than) two.

#### IV. ENCODING INFORMATION VIA CONTROLLING CHAOS

##### A. Choosing a partition and an appropriate set of symbols

Partitions give a rule which assigns a symbol whenever the state is in a certain portion of the phase space. For the return map in Fig. 3(b), a natural way to choose the partition is to divide the map at its maximum, so that the left side corresponds to “0” and the right-hand side to “1.” Such a partition rule is often called a *two-level quantizer*. Note, however, that this partition rule is not robust with respect to assigning correct symbols near the maximum of the curve; i.e., noise or a small error in measuring  $|R_m|$  will result in an incorrect symbol assignment. To make our communication system robust to noise, we will introduce a “noise-resisting gap” (Sec. IV C). That is, we restrict the dynamics so that the orbit never falls within an interval of width  $2\Delta R$  centered at the maximum of the curve in Fig. 3(b) (e.g., Ref. 15).

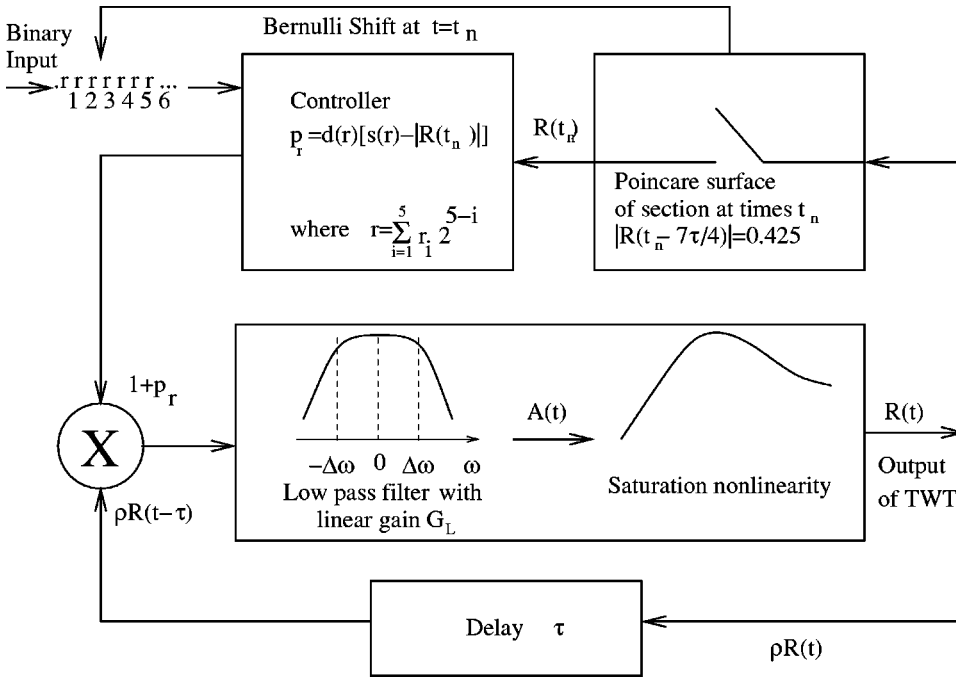


FIG. 4. Schematic of the controller.

**B. Learning the grammar of the symbolic dynamics of the system (which symbol sequences are allowed)**

Starting off with a particular value of  $|R_m|$  and iterating the map  $N - 1$  times forward, one obtains a binary string of length  $N$ ; examining many such strings originating from different initial conditions gives the collection of binary strings of length  $N$  allowed by the dynamics. Such a collection forms the symbolic grammar of the system. In what follows, to transmit a message consisting of an arbitrary sequence of bits, we code the message in such a way that in can be represented as a different bit string (possibly of length greater than its original length) such that any substring of length  $N$  (with  $N$  suitably chosen) within this new string does not violate the grammar restrictions of the free running system.

**C. Encoding information by means of controlling the symbolic dynamics**

For dynamics as in Fig. 3, techniques for encoding binary data by controlling chaos have been described in a number of papers.<sup>4,5,15,16</sup> The main idea is to utilize the exponential divergence of the flow by applying tiny perturbations to the system in such a way as to cause a prescribed symbolic sequence to be followed.

The method can be split into two parts.<sup>4,5,15,16</sup>

**1. Learn the dynamics of the free-running system**

Letting the flow for our system (2) evolve in time, we record  $|R_m|$  along with the bit string of length  $N$  following this  $|R_m|$ . (In our numerical examples we use  $N = 5$ .) A convenient way to represent this bit string is to assign to  $|R_m|$  an integer number  $n$  between 0 and  $2^N - 1$ . For our system all the  $|R_m|$ 's leading to the same bit sequence  $n$  fall within a narrow interval. Taking the averages  $s(n)$  of the  $|R_m|$  values in the interval corresponding to  $n$ , we obtain a table  $s(n)$ .

Thus, if we can set  $|R|$  to  $s(n)$ , the orbit will follow the bit sequence  $n$  on the surface of section. For example, in the case when we are willing to increase immunity to noise by means of using a “noise-resisting gap,” we only consider bit strings of a length  $N$  that never enter the gap. This, of course, introduces additional grammar restrictions. For example, in the case where the gap width is  $2\Delta R = 0.01$ , the sequence “00000” must be ruled out when message coding is done.

**2. Learn the dynamics of the perturbed system**

We now apply a small reference perturbation of amplitude  $p_{ref}$  to the system after every  $N$  crossings of the surface of section. Following an orbit for a long time, we record the values of  $|R_m|$  just before the perturbation and note the bit string  $n$  that they lead to. Averaging such values we obtain a second table,  $w(n)$ . Thus the quantity  $w(n)$  is simply a perturbed version of  $s(n)$ . In our numerical experiments the reference perturbation is a small pulse of fixed duration and amplitude applied to the input of the TWT. Having found  $s(n)$  and  $w(n)$  and assuming that the effect of the small perturbation is linear, we now make the orbit follow a desired sequence  $n_0$  by applying a perturbation of amplitude,

$$p = [|R_i| - s(n_0)]d(n_0),$$

where

$$d(n) = \frac{p_{ref}}{w(n) - s(n)}.$$

An overall view of the encoding scheme is represented pictorially in Fig. 4. The controlled attractor is shown in Fig. 5. Note that by construction, any segment of the controlled orbit of a length  $N$  (and, therefore, the whole orbit) avoids the noise-resisting gap of width  $2\Delta R$  indicated in Fig. 3(b). Therefore, the controlled orbit will also avoid all the post images of that gap. Thus, as compared to the attractor in Fig. 3, the controlled attractor (Fig. 5) is permeated by gaps.

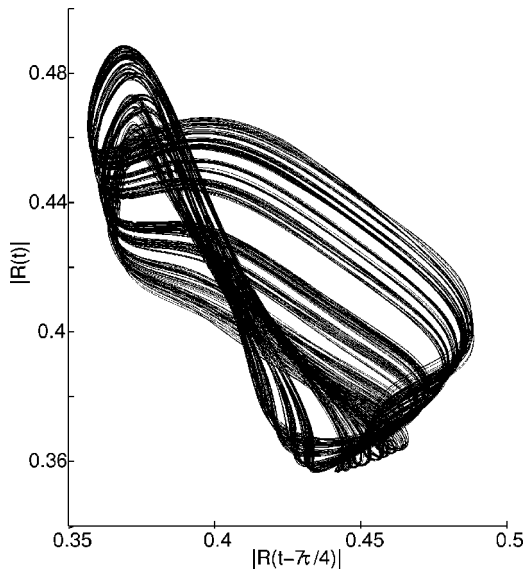


FIG. 5. Controlled attractor for  $N=5$  and gap size  $2\Delta R=0.01$ . A random sequence of bits was used for generating the message.

**V. SYNCHRONIZATION AND RETRANSMISSION**

TWT's are commonly used in satellite communication systems. As an example, we imagine that the encoded chaotic signal generator described in Sec. IV is transmitting from a ground-based station to a satellite. We wish to receive a signal on the satellite, amplify it, and retransmit it back to the ground.

In our communication system we attempt to use another TWT that is an identical (or nearly identical) replica of the original TWT to amplify and retransmit the received signal. Using a low power pre-amplifier, we envision restoring the signal from the receiving antenna to the (small) amplitude  $\rho R$  at the input of the transmitting TWT. Ideally (in the absence of noise and channel distortion) the input to the TWT on the ground (from the feedback) and the TWT on the satellite (from the preamplifier) will be identical. Thus they produce identical outputs, and the TWT on the satellite ac-

complishes distortionless amplification to high power even though it is operating in a fully nonlinear regime. (This scheme may be regarded as a variant on ideas related to the synchronization of chaotic systems.<sup>6-8</sup>)

Note that this type of synchronism-based system is only possible because our information-bearing controlled signal is one of the naturally occurring chaotic orbits of the original transmitting TWT. We have also tested the robustness of our amplification scheme to noise (see Fig. 6).

We believe that such a system offers potential advantages with respect to compactness, an important consideration for a satellite system where weight is a prime concern. Also, there is some indication that TWT's operated in the chaotic regime may have enhanced power efficiency as compared to TWT's operating in their stable linear range.<sup>2</sup> This again may be advantageous since the need for the expulsion of waste heat from the satellite is lessened.

**VI. NOISE ANALYSIS**

We consider three issues: (1) bandwidth efficiency, (2) bit error rate (BER) dependence on signal-to-noise ratio (SNR), and (3) the effect of synchronization on SNR.

(1) *Bandwidth efficiency.* Bandwidth efficiency is defined as the ratio of the bit rate to the signal bandwidth. The bit rate is determined by the number of crossings of the Poincaré plane per unit time and is approximately 0.5 bits per unit of our normalized time variable; the bandwidth can be estimated as the portion of the power spectrum of the signal (see Fig. 7) containing 99% of total power, which is approximately 1. Therefore, the bandwidth efficiency is approximately 0.5. For comparison, the bandwidth efficiency of a binary PSK (phase shift keying)<sup>17</sup> or FSK (frequency shift keying)<sup>17</sup> modulated signal is 0.5. Thus, our scheme uses bandwidth at least as efficiently as some traditionally used modulation techniques. (Detailed information on different types of modulation techniques and their properties can be found in Ref. 17.)

(2) *BER dependence on SNR.* An upper bound for BER

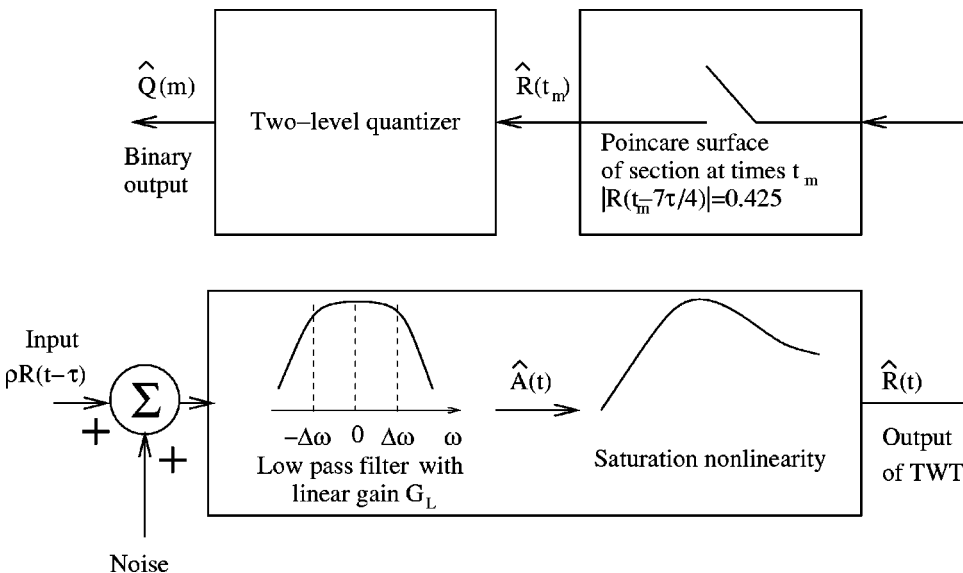


FIG. 6. Schematic of the receiver.

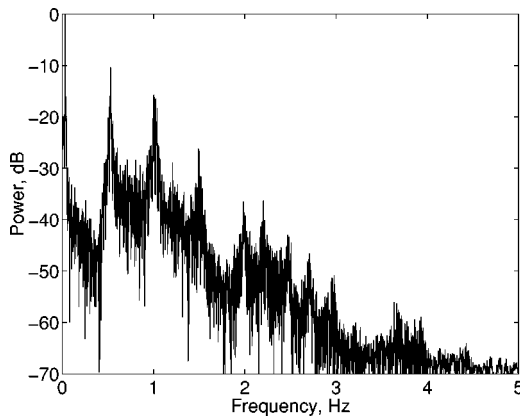


FIG. 7. Normalized power spectral density of the transmitted signal.

(assuming that “0”s and “1”s are equally likely to occur) is derived in the Appendix and is given by

$$P_e \leq \frac{1}{2} \operatorname{erfc} \left( \frac{\Delta \hat{R}}{\sqrt{N_0 f_B}} \right) < \frac{e^{-(\Delta \hat{R})^2 / N_0 f_B}}{2\sqrt{\pi}},$$

where  $f_B$  is the bandwidth of the signal,  $\Delta \hat{R}$  is a noise-resisting gap of the received chaotic attractor (signal), and  $N_0$  is the noise power spectral density at the receiver input. Thus the BER becomes very small for  $(\Delta \hat{R})^2 \gg N_0 f_B$ . Note that  $N_0 f_B$  represents the effective power of the interfering signal (noise), whereas  $(\Delta \hat{R})^2$  is determined by the relative size of the noise-resisting gap as well as the overall size of the chaotic attractor (signal strength or power, speaking in practical terms) at the receiver input. Therefore, there exist two ways of improving BER performance: boosting the signal power, and increasing the relative size of the noise-resisting gap. A bigger gap requires a more restricted symbolic dynamics; therefore, less data can be sent. While the output power of TWT is limited by its physical design, the gap size can be controlled by altering the symbolic dynamics<sup>15</sup> of the TWT, and therefore, offers a rather flexible means of tuning a chaotic TWT for either better BER performance or a higher data rate.

(3) *Effect of synchronization on SNR.* In our numerical tests we added to the chaotic signal a filtered low-frequency Gaussian noise component with a frequency bandwidth of approximately 1. In this case, the cutoff frequency of the linear component in our TWT model (see Fig. 1) will lie beyond the bandwidth of the noise component, and therefore, the linear low-pass portion of our TWT model will not filter incoming noise. In this scenario, any improvement in BER performance must be attributed to the effect of synchronization. Numerical simulations show that the SNR after synchronization (SNR at the output of the receiving TWT vs SNR at the receiving antenna) increases by approximately 11.3 dB.

Another set of numerical simulations showed that the BER at the output of the synchronized TWT was an order of magnitude less than that at the input of the receiving TWT for an input SNR equal to 32 dB. The time series that illustrates the effect of synchronization are shown in Fig. 8.

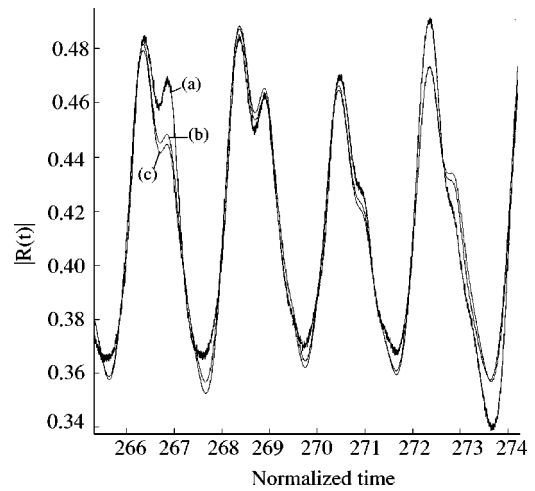


FIG. 8. Time series of an (a) noisy chaotic signal, (b) chaotic signal prior to adding noise, and (c) the signal filtered by means of chaotic synchronization (c). One can clearly see that time series (c) and (b) look almost indistinguishable, even though time series (a) is quite different.

An important issue relevant to the overall performance of our communication scheme concerns the optimal gap size  $\Delta R$ . As we have shown earlier,  $\Delta R$  can be viewed as a variable that allows one to optimize a given chaotic communication system for a particular application, or meet certain design constraints. One such constraint could be a given threshold for BER. Another constraint could be to maximize information throughput (data with no errors) of the TWT-based chaotic communication system. Unfortunately, there is no clear relation between information throughput and the size of  $\Delta R$ . Although increasing  $\Delta R$  greatly improves robustness to noise, the entropy of the map describing dynamics of the TWT decreases, and the effective data rate in the communication system also decreases. On the other hand, the channel coding theorem<sup>17</sup> states that there exists an error control coding algorithm such that the probability of an error can be made smaller than any  $\epsilon > 0$  provided that the code rate is smaller than channel capacity  $C$ . In other words, the channel capacity  $C$  determines an upper bound on the amount of error-free information that can be sent through the channel. So the answer can be found by looking at the gap size, bit rate, and SNR in a more general way: the optimum gap size in this case would simply maximize the channel capacity  $C$  for a given value of the noise power density at the receiver input.

To summarize the results of this section, we addressed two key components of communication system design, bandwidth efficiency and performance in a noisy environment. We also identified a mechanism that can be used to optimize the performance of the proposed communication system.

## VII. FUTURE WORK

Summarizing our work, we have developed a model of a proposed chaotic communication system where controlling chaos is used as an alternative means of “modulation” for the encoding of binary information. We have shown using

numerical simulations that, while the proposed communication system in some aspects behaves as well as conventional ones, it also offers potentially new benefits.

We believe that our work may be relevant in situations where the main concern is increase of the compactness and power efficiency of the amplifier (as, for example, in the case where the amplifier is on a space satellite).

While traditional modulation techniques, such as PSK (phase shift keying) and QAM (quadrature amplitude modulation),<sup>17</sup> allow the avoidance of unmodulated spectral components and, therefore, achieve high power efficiency, these techniques can only be used with linear TWTs. On the other hand, TWT's in general are known to be more power efficient when operating in the nonlinear regime, when chaotic modulation can be utilized.

A qualitative analysis of the chaotic attractor in Fig. 5 reveals that the chaotic flow produced by our model can be characterized by small relative amplitude variation and the absence of rapid transitions in phase. As a result, a large fraction of spectral power is being contained in the periodic (unmodulated) spectral component. In contrast, conventional modulation techniques, such as QAM and PSK, are characterized by fast transitions in phase, which allows utilization of the transmitted energy in a very efficient manner.

We note, however, that the large unmodulated component in our numerical example is a characteristic of our particular example and not of the general proposed method. Thus it remains a problem for future study to find and characterize chaotic TWT operation that yields chaotic signals that have a smaller unmodulated component.<sup>18</sup>

Thus, it is not yet clear whether the *overall* performance of the chaotic satellite communication system that we propose is better than that of traditionally used ones. A clear answer to this question awaits experimental implementation and test of our proposed system.<sup>18</sup>

## ACKNOWLEDGMENT

This research was supported by the Naval Research Laboratory, by ONR (physics), and by the NSF (PHYS-0098632).

## APPENDIX: DERIVATION OF THE UPPER BOUND FOR BER

Let  $\hat{R}$  be a “modulated” chaotic signal  $R(t)$  received by the second TWT. Clearly,  $\hat{R}$  will be considerably attenuated. Therefore, the new attractor obtained from  $\hat{R}$  will be a scaled-down version of the one in Fig. 5. Sampling the values of  $|\hat{R}(t_n)|$  at the surface of section of the new attractor obtained from the received signal and comparing them to the value of  $\hat{R}$  at the middle of its noise resisting gap, one interprets  $|\hat{R}(t_n)|$  as either a “0” or a “1.” Due to noise in the channel, some of the bits in the receiver will be read incorrectly. We are going now to estimate the fraction of incorrectly transmitted bits or BER.

For convenience, in the following, we regard the receiving TWT as acting like a linear amplifier [i.e., we neglect the nonlinearity in (2)]. Suppose that white Gaussian noise  $w(t)$

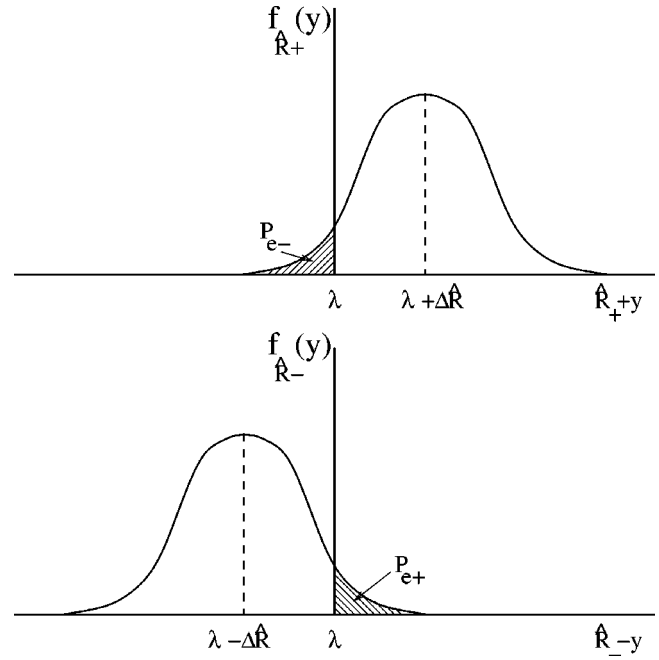


FIG. 9. Distribution of the signal sampled at the output of the low-pass filter with the cutoff frequency  $\omega_0$ .

with the power spectral density  $N_0/2$  is added to the signal at the receiver input. We model the effect of the slow wave structure of the receiving TWT as a first-order low-pass filter. What we sample at the output of the receiving TWT is a true signal  $|\hat{R}(t_n)|$  plus  $y(t_n)$ , where  $y(t) = \int_{-\infty}^{\infty} h(\tau)w(t - \tau)d\tau$ . For the first-order low-pass filter with cutoff frequency  $\omega_0$ ,  $h(t) = \omega_0 u(t)e^{-i\omega_0 t}$ , where  $u(t)$  is a step function. Now we make another assumption; we assume that, in the absence of noise,  $|\hat{R}(t_n)| = \hat{R}_{\pm} = \lambda \pm \Delta \hat{R}$ . In other words, we assume that the signal is always measured at the edge of the noise-resisting gap, where the value of the measured signal is closest to the threshold  $\lambda$  and, thus, errors are the most likely to occur. Therefore, we are going to estimate an upper bound for the BER. Since errors occur due to  $y(t)$ , and since  $y(t)$  is a Gaussian process, we would like to find the variance of  $y(t)$ :

$$\begin{aligned} \sigma_y^2 &= E[y^2] \\ &= \omega_0^2 E \left[ \int_0^{\infty} \int_0^{\infty} e^{-\omega_0 \tau_1} e^{-\omega_0 \tau_2} w(t - \tau_1) w(t - \tau_2) d\tau_1 d\tau_2 \right] \\ &= \omega_0^2 \int_0^{\infty} \int_0^{\infty} e^{-\omega_0 \tau_1} e^{-\omega_0 \tau_2} E[w(t - \tau_1) w(t - \tau_2)] d\tau_1 d\tau_2 \\ &= \omega_0^2 \int_0^{\infty} \int_0^{\infty} e^{-\omega_0 \tau_1} e^{-\omega_0 \tau_2} R_w(t - \tau_1, t - \tau_2) d\tau_1 d\tau_2. \end{aligned}$$

The autocorrelation function of  $w(t)$  is  $R_w(\tau_1, \tau_2) = N_0/2 \delta(\tau_1 - \tau_2)$ , so the integral above becomes

$$\sigma_y^2 = \omega_0^2 \int_0^{\infty} e^{-2\omega_0 \tau_1} d\tau_1 = \frac{N_0 \omega_0}{4}.$$

Remembering that  $y(t)$  is a Gaussian process, the pdf of  $\hat{R}_\pm + y(t_n)$  can be expressed as

$$f_{\hat{R}_\pm}(y) = \frac{1}{\sqrt{\pi N_0 \omega_0 / 2}} \exp\left(-\frac{(y + \lambda \pm \Delta \hat{R})^2}{N_0 \omega_0 / 2}\right)$$

(see Fig. 9). Here  $\pm$  refers to the condition that a “1” or a “0” was transmitted [ $\hat{R}_+ + y(t_n)$  or  $\hat{R}_- + y(t_n)$  was received, respectively].

For the case of noncoherent detection (when we do not know at what times the signal needs to be sampled), the effective width of a Gaussian becomes twice of that of the coherent case described above. Therefore,

$$f_{\hat{R}_\pm}^{\text{noncoh}}(y) = \frac{1}{\sqrt{\pi N_0 \omega_0}} \exp\left(-\frac{(y + \lambda \pm \Delta \hat{R})^2}{N_0 \omega_0}\right).$$

The probability of an event in which the received symbol is different from what was transmitted is

$$\begin{aligned} P_{e\pm} &= \int_{\lambda}^{\pm\infty} f_{\hat{R}_\pm}(y) dy \\ &= \frac{1}{\sqrt{\pi N_0 \omega_0}} \int_{\lambda}^{\pm\infty} \exp\left(-\frac{(y + \lambda \pm \Delta \hat{R})^2}{N_0 \omega_0}\right) dy. \end{aligned}$$

Performing integration one gets a rather simple answer:

$$P_e = P_{e\pm} = \frac{1}{2} \operatorname{erfc}\left(\sqrt{\frac{(\Delta \hat{R})^2}{N_0 \omega_0}}\right). \quad (\text{A1})$$

Equation (A1) gives an upper bound for BER.

- <sup>1</sup>A. H. W. Beck, *Velocity-Modulated Thermionic Tubes* (Cambridge University Press, Cambridge, 1948).
- <sup>2</sup>J. F. Gittins, *Power Travelling-Wave Tubes* (American Elsevier, New York, 1965).
- <sup>3</sup>J. R. Pierce, *Traveling Wave Tubes* (Nostrand, Princeton, NJ, 1950).
- <sup>4</sup>S. Hayes, C. Grebogi, and E. Ott, Phys. Rev. Lett. **70**, 3031 (1993).
- <sup>5</sup>S. Hayes, C. Grebogi, E. Ott, and A. Mark, Phys. Rev. Lett. **73**, 1781 (1994).
- <sup>6</sup>L. Pecora and T. Carroll, Phys. Rev. Lett. **64**, 821 (1990).
- <sup>7</sup>K. Cuomo and A. Oppenheim, Phys. Rev. Lett. **71**, 66 (1993).
- <sup>8</sup>L. Kocarev and U. Parlitz, Phys. Rev. Lett. **74**, 5028 (1995).
- <sup>9</sup>A. A. M. Saleh, IEEE Trans. Communications **29**, 1751 (1981).
- <sup>10</sup>M. C. Jeruchim, P. Balaban, and K. S. Shanmugan, *Simulation of Communication Systems* (Plenum, New York, 1992).
- <sup>11</sup>T. M. Antonsen, Jr. and B. Levush, “CHRISTINE: A multifrequency parametric simulation code for traveling-wave tube amplifiers,” NRL Report 97-9845, 1997.
- <sup>12</sup>D. K. Abe, M. T. Ngô, B. Levush, T. M. Antonsen, Jr., and D. P. Chernin, IEEE Trans. Plasma Sci. **28**, 576 (2000).
- <sup>13</sup>J. G. Wöhlbier, J. H. Booske, and I. Dobson, “New nonlinear multifrequency TWT model,” 2nd IEEE International Vacuum Electronics Conference, Huis ter Duin, Noordwijk, Netherlands, 2–4 April 2001.
- <sup>14</sup>E. Ott, *Chaos in Dynamical Systems* (Cambridge University Press, Cambridge, 1993), Chap. 4.
- <sup>15</sup>E. Bolt and M. Dolnik, Phys. Rev. E **55**, 6404 (1997).
- <sup>16</sup>E. Ott, C. Grebogi, and J. A. Yorke, Phys. Rev. Lett. **64**, 1196 (1990).
- <sup>17</sup>S. Haykin, *Communication Systems* (Wiley, New York, 1994).
- <sup>18</sup>We have also obtained preliminary results of numerical modeling for a second order model in which the linear part of the TWT is modeled with a second order maximally flat filter (which would be a more precise description of a real TWT). With the second order filter, Eq. (2) is modified by the addition of a term  $d^2A(t)/dt^2$  on the left-hand side. For a certain set of model parameters we observe again a low-dimensional chaotic flow which can be controlled using the technique described above for a first-order model. Now, however, the phase of the signal changes more sporadically. This results in a much smaller carrier power (11% of the total signal power as compared to 70% for the first order model) and, therefore, higher power efficiency.